IF/P-06

Implosion Scaling and Hydrodynamically Equivalent Target Design - Strategy for Proof of Principle of High Gain Inertial Fusion -

M. Murakami, K. Nishihara, H. Azechi, M. Nakatsuka, T. Kanabe, N. Miyanaga

Institute of Laser Engineering, Osaka University, Suita, Osaka 565-0871, Japan

e-mail contact of main author: mym@ile.osaka-u.ac.jp

Abstract. Scaling laws for hydrodynamically similar implosions are derived by applying Lie group analysis to the set of partial differential equations for the hydrodynamic system. Physically this implies that any fluid system belonging to a common similarity group evolves quite in the same manner including hydrodynamic instabilities. The scalings strongly depend on the description of the energy transport, i.e., whether the fluid system is heat conductive or adiabatic. Under a fully specified group transformation including prescriptions on the laser wavelength and the ionization state, the hydrodynamic similarity can still be preserved even when the system is cooperated with such other energy sources as classical laser absorption, hot electrons, local alpha heating, and bremsstrahlung loss. The results are expected to give the basis of target design and diagnostics for scaled high gain experiments in future.

1. Introduction

Aiming at ignition in inertial fusion energy (IFE) development, the National Ignition Facility (NIF) in the U.S. [1] and the Laser Mega Joule (LMJ) in France [2] are now under construction with a driver energy of about 2 MJ. Meanwhile, at the Institute of Laser Engineering, Osaka University, the project, fast ignition realization experiments (FIREX), has been proposed for the proof of principle of high gain IFE. A goal of FIREX is to address the equivalent physics of confinement (EPOC) under a scaled (miniature) design. One should know then how to design such a miniature system and to judge to which extent the two systems are equivalent to each other. So far, many target designs have been made by employing a most simple and conventional scaling, which relates two hydrodynamically equivalent implosions (HEI) under the adiabatic assumption. In a realistic system, however, heat conduction cannot be neglected. Therefore, the present work takes the heat conductivity into account as the new ingredient, and shows that the resultant scaling laws for heat conductive fluids and adiabatic fluids are substantially different from each other.

A most simple and conventional scaling between two similar implosions would be in the following form: radius $r' = \xi r$, mass $M' = \xi^3 M$, and energy $E' = \xi^3 E$, where the primes denote the physical quantities in the scaled system related by the scale factor ξ with the parent system without prime. In this case, velocity $v' = (E'/M')^{1/2} = v$, density $\rho' = M'/r'^3 = \rho$, temperature $T' = E'/M' = T$, and energy flux $I' = E'^{3/2}/r'^3 M'^{1/2} = I$ are all kept invariant. However, in the following, this conventional scaling law, which is not beyond the simple dimensional analysis, turns out to be valid only for a specific case and be inappropriate for systems where thermal conduction plays an important role.

Lie group analysis [3] which is employed in the present work, is not only a powerful method to seek self-similar solutions of partial differential equations (PDE) but also a unique and most adequate technique to extract the group invariance properties of such a PDE system. Coggeshall and Axford [4] published their extensive and thorough study on radiation hydrodynamics equation by means of the Lie group analysis, in which they focused to find the self-similarities. Their work contrasts with our present work, which is mainly devoted to find the mutual-similarities. It should be also noted that Basko and Johner [5] made use of the group invariance properties of the pure hydrodynamic system under the adiabatic assumption

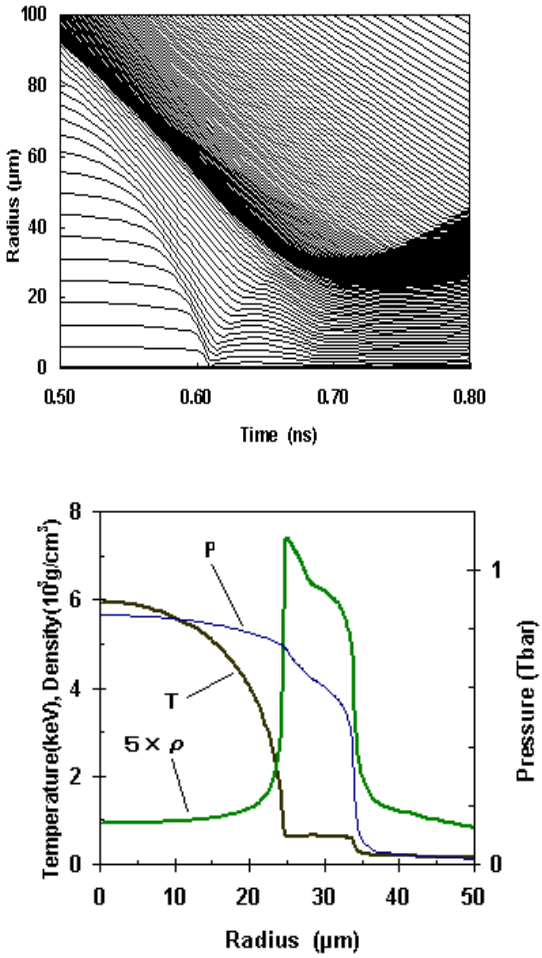

FIG.1. Flow diagram of the parent system (top), and the spatial profiles of the core plasma (bottom) at peak compression.

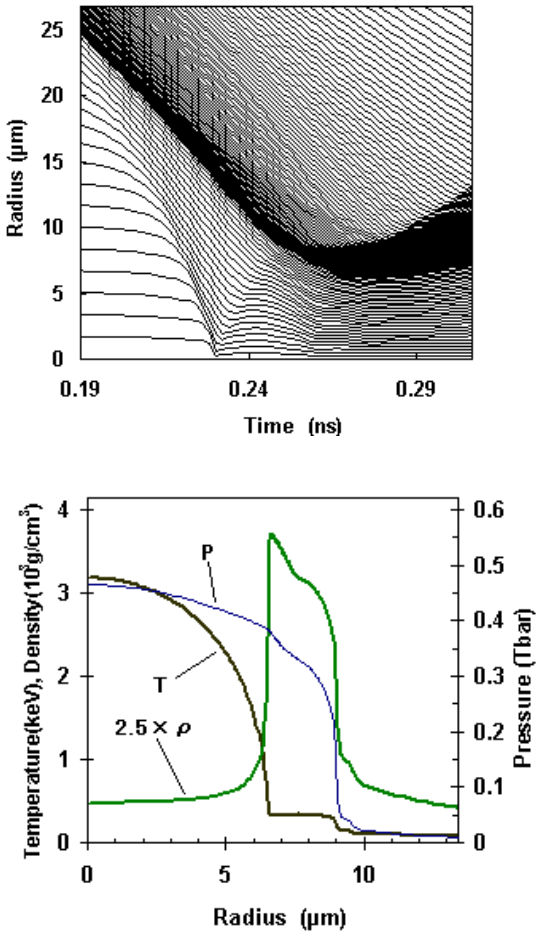

FIG.2. Flow diagram of the scaled system (top), and the spatial profiles of the core plasma (bottom) at peak compression.

to derive an ignition energy scaling. In a more realistic system, however, thermal conduction cannot be neglected particularly in implosions forming a hot spot at the target center, because it substantially affects not only the one-dimensional back ground dynamics but also multidimensional hydrodynamic instabilities. The present work takes the thermal conductivity into account as the new ingredient and shows that the resultant scaling laws for thermal conductive fluids and adiabatic fluids are substantially different from each other [6].

2. Symmetry Analysis

The goal of the present work is to find an appropriate group transformation between two HEI in different sizes. Such information is indispensable at any cost for the right target design with reduced scales. It is then inevitable to analyze the group invariance properties of a given set of PDE describing the hydrodynamics of the system. In the analysis, we introduce such a group transformation characterized by the scale factor x: radius $r' = \xi r$, time $t' = \xi^a t$, velocity $v' = \xi^b v$, temperature $T' = \xi^c T$, density $\rho' = \xi^d \rho$, where a, b, c, and d are unknown constants. Substituting these transformed variables for the mass, momentum, and energy equations, these four constants can be determined in such a manner that the system can be preserved invariant. Here, the heat conductivity in the energy equation is approximately given in the power law form, $\kappa = \kappa_0 T^n/\rho^m$, with κ_0, m, and n being constants. Electron heat conductivity, for example, corresponds to m = 0 and n = 5/2. Substituting the above anzats for the

hydrodynamic PDE, one can obtain the scaling law of HEI [6].

3. Simulation Results

As the initial configuration of the parent system, we employ that used in Ref. [5], which gives an analytical form for the profile of imploding deuterium-tritium (DT) plasma in flight at its peak velocity. The DT plasma is composed of the central gas and the surrounding dense shell, and the whole profile is fully specified by six parameters. There is no external pressure imposed on the plasma, and therefore the system evolves in a self-sustained manner. We do not elaborate more details, because such detailed information does not matter at all in discussing the HS property throughout this paper. Figure 1(a) shows the flow diagram of the parent implosion around its peak compression, while Fig. 1(b) shows the profiles of the temperature, density, and pressure at the peak compression (t ~ 0.7 ns).

Next, we conduct scaled simulations to compare with the parent case, where two different cases, (A) electron heat conduction and (C) no heat conduction, are chosen. Each of them is further specified for the two different energy scales, μ = 1 % and 10 %. Figures 2(a) and 2(b) respectively show the flow diagram and the plasma profiles at the peak compression for the μ = 1 % case. Figures 1 and 2 look quite similar to each other. As will be shown below, the

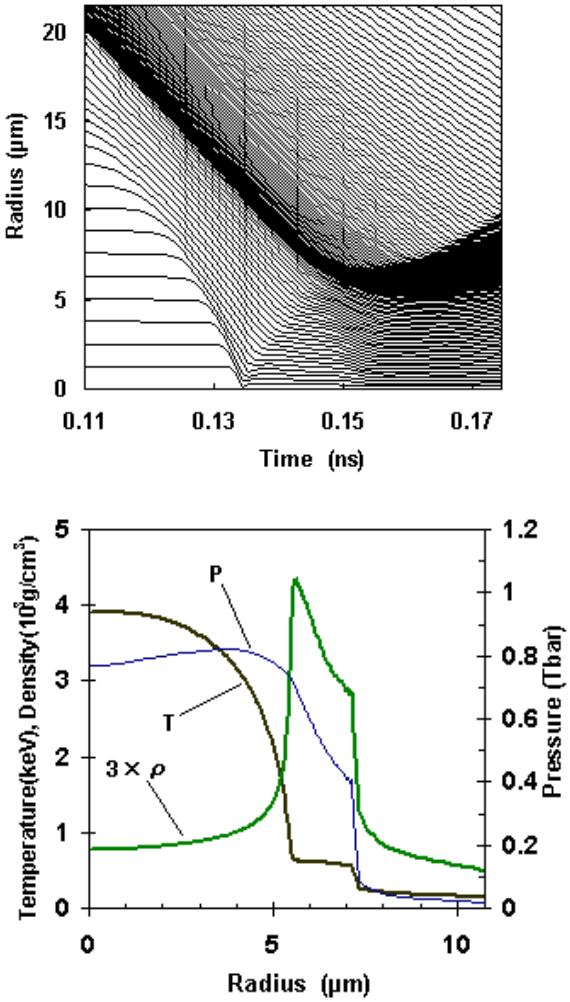

FIG.3. Flow diagram of the scaled implosion (μ=0.01) without thermal conduction (top) and spatial profiles at peak compression (bottom)

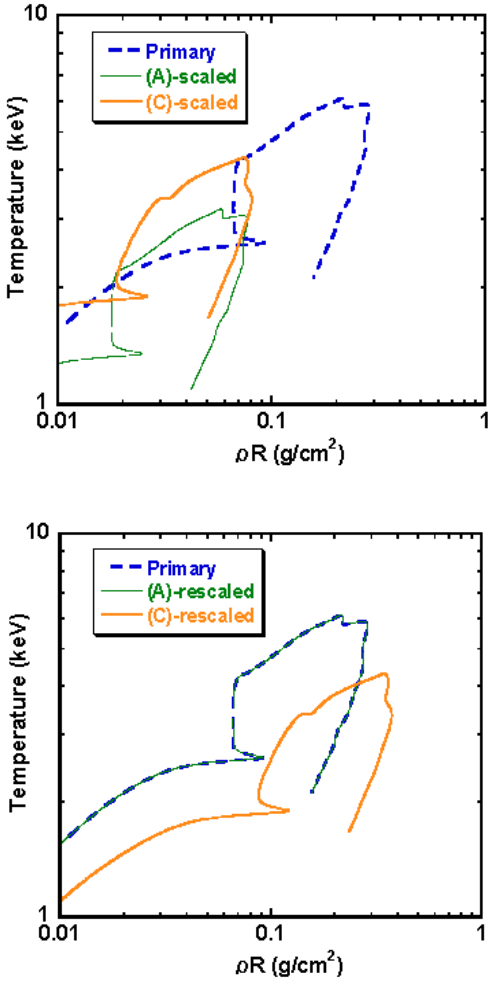

FIG.4. Temporal evolution of T and ρR (top) corresponding to the cases in Figs.1-3 and the rescaled version (bottom).

TABLE I: TARGET AND PLASMA PARAMETERS FOR HGX AND EPOC

Physical quantity	HGX (100%)	EPOC1(3%)	EPOC2 (0.3%)
1. Laser			
Energy	2.0 MJ	60 kJ	6.0 kJ
Power	300 TW	19 TW	3.1 TW
Intensity	9.0 10^{14} W/cm^2	4.2 10^{14} W/cm^2	2.6 10^{14} W/cm^2
Pulse width	5.0 ns	2.4 ns	1.4 ns
2. Target & Implosion			
Fuel mass	1.5 μg	74 μg	10 μg
Initial radius	2.0 mm	0.73 mm	0.38 mm
Ablation pressure	90 Mbar	55 Mbar	39 Mbar
Implosion velocity	3.3 10^7 cm/s	2.6 10^7 cm/s	2.2 10^7 cm/s
3. Confinement			
Spark temperature	5.0 keV	3.0 keV	2.2 keV
ρ_{max}/ρ_{solid}	2300	2300	2300
ρ_{hot}/ρ_{solid}	250	250	250
ρR (hot spot)	0.31 g/cm^2	0.11 g/cm^2	59 mg/cm^2
ρR (hot+cold fuel)	1.8 g/cm^2	0.66 g/cm^2	0.34 g/cm^2
Spark radius	60 μm	22 μm	11 μm
Convergence ratio	33	33	33

Density is the physical quantity which is kept invariant. EPOC1 and EPOC2 are scaled cases at 3% and 0.3% energy level of the parent case, HGX.

scaled simulation results agree precisely with the predictions obtained by the model, and therefore it can be concluded that they are rigidly hydrodynamically similar to each other.

Figure 3 is for case (C) just as Figs. 2(a) and 2(b), that is, they are based on the specified adiabatic scaling with c = d = 0. At a glance, the patterns of the flow diagram and the spatial profiles in Fig.3 look similar to those in Figs.1 and 2. Then, one might think "What is wrong? Although the patterns in Fig.3 are not exactly the same as those in Fig.2, they indeed look similar, so that the specified adiabatic scaling can be acceptable as well." However, what is required for a right scaling is both to prescribe scaled target designs and to predict resultant plasma characteristics. Scaling (C) and the simulation results in Fig.3 are in unacceptable contradiction to each other. Therefore the adiabatic scaling is apparently inappropriate for such a system that the heat conduction is taken into account.

The above argument can be well illustrated in terms of the ρR-T diagram given in Fig. 4(a), which shows the temporal evolutions of the mass-averaged temperature T versus the areal mass density of the hot spot ρR for the three cases presented in Figs. 1-3. In the numerical simulations, the hot spot surface was identified in such a manner that the heat flux has its maximum on the surface. The overall behavior on the ρR-T diagram can be explained by comparing with the flow diagram as follows. Note that we here use the parent case as an example (compare Fig. 1(a) and the thick dashed curve in Fig. 4(a). In the early stage (t < 0.6 ns), both ρR and T increase monotonically with time. Meanwhile, the converging shock wave transmitting through the unperturbed central gas accelerates continuously. At the shock front, the gas is first compressed up to $4\rho_0$ (ρ_0 is the initial unperturbed gas density) and further compressed adiabatically. On the collapse at t = 0.61 ns, the density profile in the vicinity of the target center becomes uniform, and ρR value quickly increases keeping T almost constant. As a result, ρR reaches its local maximum, which can be observed as the tip of the notch at ρR = 0.95 g/cm2 and T = 2.6 keV in Fig. 4(a). The reason of the slight decrease in ρR after the collapse is attributed to the abrupt change of the density profile. On the collapse, the reflected

shock begins to transmit outward. Therefore the central mass tends to be wiped out.
Since the three curves are the raw data of the simulations, it is hard to judge which curve, (A) or (C), is correctly scaled. For a better comparison, therefore, we rescale the both curves in Fig. 4(a) in such a manner that they are shifted in the direction of each axis by the reciprocal factors, $\rho R/\rho' R'$ and T/T', to see whether the parent curve can be really reproduced. Figure 4(b) shows the rescaled version of Fig. 4(a) thus made. As can be easily seen, the (A)-rescaled curve exactly fits the parent curve, while the (C)-rescaled curve conspicuously fails to reproduce the parent curve. Although the two scaled curves in Fig. 4(a) look somewhat similar to each other, they are not the same actually; this means that they cannot be in the common HSI group. These consequences tell that the scaling law based on the adiabatic assumption is by no means appropriate for the heat conductive fluids.

4. EPOC Scaling for High Gain Targets

The strategic principle to address the EPOC is as follows: To prove that a miniature experiment (EPOC1) and an expected high gain experiment (HGX; not conducted actually) are equivalent according to the scaling model, it is necessary to demonstrate a pair of scaled implosion experiments (EPOC 1 and 2) under the same system (E_L = 60 kJ, λ_L = 0.35 μm, N_B = 92 beams) and to show that they are indeed self-consistent with the model prediction. Table I shows the comparison of various physical parameters for three different implosion cases obtained from the scaling model described above; the first column shows the parameters expected for a HGX, and the other two columns are for the energy scaled versions with the scale factors of 3% (EPOC1) and 0.3% (EPOC2). These results will give the basis of the target fabrication and diagnostics for the experiments on FIREX.

5. Summary

Scaling laws for the hydrodynamically similar implosions have been derived by applying the Lie group analysis to the set of PDE for the hydrodynamic system, taking the heat conductivity into account as the new ingredient. The scaling laws for thermal conductive fluids are conspicuously different from those for adiabatic fluids. The former has one less freedom than the latter due to the additional constraint - thermal conductivity. The scaling laws obtained analytically have been confirmed by the numerical simulations.

HSI property is most likely preserved under the fully specified group transformation including the prescriptions on the laser wavelength and the ionization state even when the system is cooperated with such other energy sources as classical laser absorption, hot electrons, local alpha heating, and bremsstrahlung loss. As for the dual heat conduction system, just incidentally, there is no solution to achieve HSI under both the electron heat conduction and the radiation heat conduction. Full HSI experiments taking all the above effects into account are not realistic in the rigorous sense. However, some elemental HSI experiments, focusing on each specific phase of an implosion, are expected to be feasible and to give the basis of target design and diagnostics for scaled high gain experiments in future.

References

[1] CAMPBELL, E.M. and HOGAN, W.J., Plasma Phys. Controlled Fusion **41** (1999) B39.
[2] JOLAS, A., BAYER, C., Edattolo *et al., Inertial Fusion Sciences and Applications 99* (Edited by LABAUNE, C., HOGAN, W., and TANAKA, K.A., Elsevier, 2000), pp.68-73.
[3] LIE, S., *Theorie der Transformationsgruppen* (Chelsea, New York, 1970).
[4] COGGESHAL, S.V. and AXFORD, R.A., Phys. Fluids **29** (1986) 2398.
[5] BASKO, M.M. and JOHNER, J., Nucl. Fusion **12** (1998) 1779.
[6] MURAKAMI, M. and IIDA, S., Phys. Plasmas **9** (2002) 2745.